Proceedings of the 9ICEG
9th International Congress on Environmental Geotechnics
25-28 June, 2023 | Chania, Greece

https://doi.org/10.53243/ICEG2023-123

Study on modelling of compacted Bentonite under wetting and drying cycles

S. Sato[1], T. Shirakawabe[2], S. Yamamoto[3], T. Shimura[4] and T. Nishimura[5]

[1] *Manager, PhD, Obayashi corporation, Tokyo, Japan, email: sato.shin.ro@obayashi.co.jp*

[2] *Obayashi corporation, Tokyo, Japan, email: shirakawabe.takumi@obayashi.co.jp*

[3] *Senior general manager, Dr. Eng., Obayashi corporation, Tokyo, Japan, email: yamamoto.shuichi@obayashi.co.jp*

[4] *General Manager, Obayashi corporation, Tokyo, Japan, email: shimura.tomoyuki@obayashi.co.jp*

[5] *Professor, Ashikaga University, Tochigi, Japan, email: nishimura.tomoyoshi@g.ashikaga.ac.jp*

ABSTRACT

Bentonite used in the engineered barrier of nuclear waste disposal facilities will swell on wetting and undergoes drying caused by heat from the waste. Therefore, analyses of the engineered barrier are required to reproduce volume change with the change in saturation. In general, a hydro-mechanical coupled analysis is required taking into account the water retention properties of the soil when considering volume change with saturation. However, the soil-water characteristic properties are dependent on soil classification, dry density, etc., and relevant soil-water characteristic properties of the target materials (bentonite/silica sand of 70:30, dry density of 1.6Mg/m3) have not previously been obtained. Additionally, void ratio-suction relationships for the bentonite materials have not been elucidated. In this study, the material and soil-water characteristic properties for volume change with change in saturation have been obtained from column tests for the compacted bentonite/sand mixture. In particular, the changes in suction and void ratio during drying and wetting processes showed that bentonite without saturation history changed reversibly, and bentonite with saturation history changed irreversibly. Reproduction analysis of the controlled-suction column tests by the vapour equilibrium technique was performed using the obtained parameters to validate the modelling method.

Keywords: bentonite, soil-water characteristic curve, vapour pressure technique, vapour flow, numerical modelling, hydro-mechanical coupled analysis

1 INTRODUCTION

Bentonite used in the engineered barrier of nuclear waste disposal facilities will swell on wetting and undergoes drying caused by the heat from the waste. Therefore, analyses of the engineered barrier are required to reproduce volume change with degree of saturation change. The Barcelona Basic Model (BBM) proposed by Alonso et al. (1990) considers the volume change due to suction change, and is used in the analysis of many nuclear waste disposal projects. When using this model the soil-water characteristic curve (SWCC) and void ratio-suction relationship are needed, and the reproducibility is dependent on the accuracy of these properties. However, soil-water characteristic properties are dependent on soil classification, dry density, etc., and soil-water characteristic properties of target materials (bentonite/silica sand of 70:30, dry density of 1.6 Mg/m^3) have not previously been obtained. Additionally, the void ratio-suction relationship of the bentonite materials has not been previously elucidated. In this study, the SWCC and void ratio-suction relationship for the bentonite materials were obtained using the vapour equilibrium technique in controlled-suction tests. The simulation was performed to verify the validity of the obtained parameters. The vapour equilibrium technique in controlled-suction tests is controlled by the relative humidity of the air surrounding the specimen. For that reason, reproducible analyses need to consider evaporation, advection and diffusion (Pintado et al., 2009). Several analytical methods have been proposed to account for this (Olivella et al., 1996; Collin et al., 2002; Qin et al., 2010; Ayman, 2017; Bin et al., 2020). To check the volume change behaviour of the specimen due to the vapour exchange technique, the CODE_BRIGHT finite element code is used in this study (Olivella et al., 1994; Olivella et al., 1996), which allows the simulation of water, air and heat flow in a deformable porous media.

2 SOIL-WATER CHARACTERISTIC CURVE

2.1 Material and experimental procedures

The material used in this study is a mixture of sodium bentonite and silica sand, with a dry mass ratio of bentonite/silica sand of 70:30. The material is humidified using a spray to the target water content of 17.0 %, and is cured for at least 24 hours in order to achieve uniformity in the soil moisture distribution. The materials with various water contents are statically compacted in a stiff mold, to a target dry density of 1.600 Mg/m^3. The size of all specimens is 20.0 mm in diameter and 7.5 mm in height, which is a relatively small size for the measurement of total suction. To measure a wide range of suction(high suction to low suction), total suction of the specimen was determined (Bulut et al., 2002; Maček et al., 2013) by using WP4-T device, which is manufactured by Decagon Co Ltd as shown in Figure 1.

The experimental work includes two testing programs, to determine the SWCC. In Table 1 the main features for Case 1 and Case 2 are described including initial water content ranging from 17.0 % to 26.9 %, and influence of different saturation histories. Seven different suctions are applied to the specimen using the vapour pressure technique (Delage, 1998) with a constant water content of 17.0 % in Case 1. All specimens were placed in the glass desiccator with the salt solution that produces the required relative humidity in the enclosed space, with the suction derived theoretically from the relative humidity. The prepared suction range is from 2.8 MPa to 296 MPa, which is equivalent to 98.0 % to 11.0 % in relative humidity. The maximum suction of 296 MPa corresponding to a relative humidity of 11.0 %, is considered the end of the drying process in this study. All specimens are then subjected to change in suction without lateral confining pressure. Subsequently, during the wetting process suction of 296 MPa is reduced to 2.8 MPa. The mass of each specimen was measured, and water content calculated at each suction step during the drying and wetting processes. The results are indicated as the SWCC over a wide suction range. In Case 2, specimens with four different initial water contents: 17.0 %, 17.3 %, 24.0 and 26.9 % are prepared with a constant dry density of 1.600 Mg/m^3. The testing process considers only the drying process, with reduction in water content. Each suction step associated with a decrease in soil moisture is measured using the WP4-T.

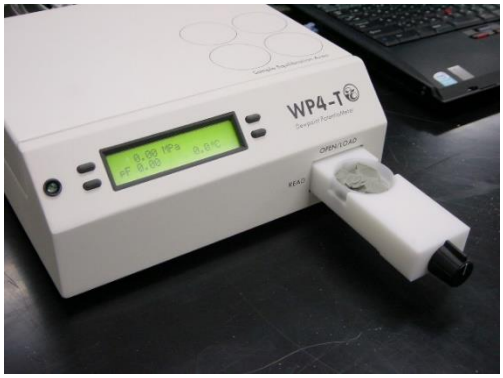

Figure 1. WP4-T device

Table 1. *Overview of experiment cases*

Case	Initial water content (%)	Water potential histories
Case 1	17.0	drying -> wetting
Case 2	17.0, 17.3, 24.0, 26.9	drying

2.2 Retention curves

SWCCs are defined as the relationship between suction and change in soil moisture, and they play a key role in the determination of unsaturated soil property functions which are used in numerical models. Suction in an unsaturated soil is considered to consist of two components; namely, matric suction and osmotic suction, and the sum of these two is equal to total suction. Matric suction is defined as the difference between the pore-air pressure and pore-water pressure. The osmotic suction (Blatz, 2008) is a function of the amount of dissolved salts in the pore fluid, and is indicated in terms of pressure in a conventional manner.

The above-mentioned soil functions can be predicted based on the SWCC. From the testing program, typical SWCCs are obtained as shown in Figure 2, which includes test results from both Case 1 and 2. In addition, the measured water content using the pressure plate technique at a suction of less than 1.0 MPa (Yamamoto et al., 2019) are included in Figure 2 as blue coloured symbols. Plotted suctions are equal to the matric suction. Yamamoto et al. (2019) conducted their tests by applying vertical stresses of 400 kPa and 200 kPa.

The constitutive model suggested by van Genuchten (van Genuchten,1980) is useful to predict the relationship between suction and degree of saturation. In this study, SWCCs are obtained using the van Genuchten (vG) model derived from the experimental data sets. The vG parameter n is confirmed as 1.32 which controls the shape of the SWCC.

The red line represents the drying process, while the black line represents the wetting process, and the degree of saturation in the drying process is larger than that during wetting for a given suction in this test. However, the difference between the drying process and wetting processes is obviously small under remaining hysteresis. It is reasonable to assume that gas pressure in void structure induces the water retention activity, and as a result, hysteresis occurs in the SWCC. For the simulation gas pressures at drying of 1.65 MPa and at wetting of 0.81 MPa were used.

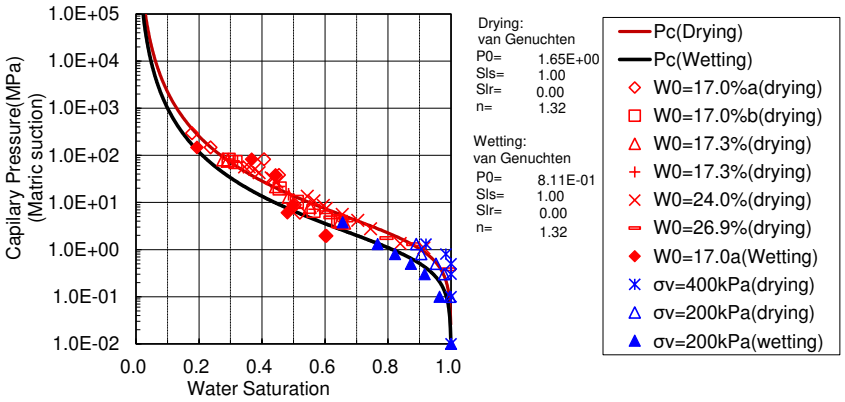

Figure 2. *Experimental dataset and the derived SWCC using a van Genuchten model.*

3 ASSESSMENT OF WETTING AND DRYING EFFECT IN CONTROLLED-SUCTION TESTS

3.1 The vapour equilibrium technique in controlled-suction tests

Tests were performed using the same materials as in Section 2.1. All specimens were statically compacted using a hydraulic jack to a height of 20.0 mm and diameter of 60.0 mm. The vapour pressure technique was used to apply suction, as described in Section 2.1. The required suction range is from 2.8 MPa to 296 MPa, controlled by using seven different salt solutions (see Section 2.1). The testing program consists of Case 1 and Case 2 with common conditions for the drying and wetting processes. The difference is in the initial condition at the beginning of the tests, with saturated condition in Case 1, and unsaturated condition in Case 2. Saturation is achieved under constant volume with height and diameter of specimen remaining constant, by absorption of distilled water. Before applying the suction control, the saturated specimen approached a degree of saturation of 100.0 %. All specimens were put into a glass desiccator with the required salt solution. Firstly, during drying from 2.8 MPa to 296 MPa suction, mass and volume are directly measured at equilibrium for each suction to calculate the parameters associated to the SWCC. Subsequently, wetting continues after the end of drying with a suction decrease to 2.8 MPa from 296 MPa. The mass and volume of the specimens are determined in the same way as during drying.

3.2 Results of the vapour equilibrium technique in controlled-suction tests

The change in degree of saturation with suction is shown in Figure 3, the saturation and suction relationship indicated irreversible behaviour between the drying and wetting processes, and confirmed hysteresis. The saturation clearly decreased with increasing suction for both Case 1 and Case 2. The saturation is less than 20.0 % or approximately 20 % when suction is 296 MPa, which is verified to be

smaller for the saturated specimen and the influence of unsaturated - saturated condition is clearly estimated. Also, the wetting process showed that the amount of hysteresis increases with reducing suction. Soil moisture changes with increasing and decreasing suction as indicated by the SWCC in Figure 4. For the saturated specimen, high water retention is observed at first suction control (i.e., suction of 2.8 MPa) in comparison with the unsaturated specimen. The calculated water content is less than 5.0 % when suction is 296 MPa, which is the driest condition. Then, water content is increased with hysteresis phenomena and constant slope on logarithmical scale. It is notable that similar increases were observed for both Cases 1 and 2.

Finally, considering void ratio and drying process an interesting phenomenon was noted. The specimen with saturation history produced a large reduction in void ratio as shown in Figure 5, it is significantly greater than that of the specimen without saturation history. The calculated slope of void ratio decrease for the specimen with saturation history is over 1.7 times that for the specimen without saturation history. Void ratio is less than 0.5 for the saturated specimen at suction of 296 MPa, while it is 0.58 for the unsaturated specimen. Void ratio increases smoothly during wetting, and swelling phenomena are observed with hysteresis. The predicted swelling index is 0.03 showing that it is not influenced by saturation hysteresis.

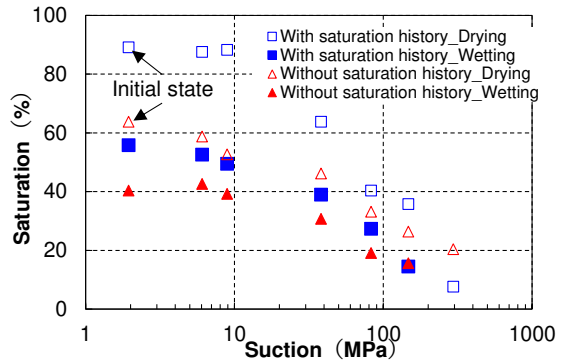

Figure 3. *Relationship of saturation and suction*

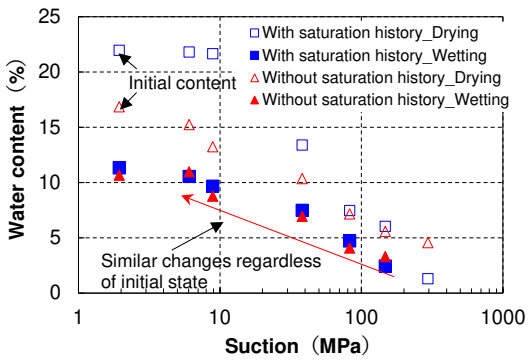

Figure 4. *Relationship of water content and suction*

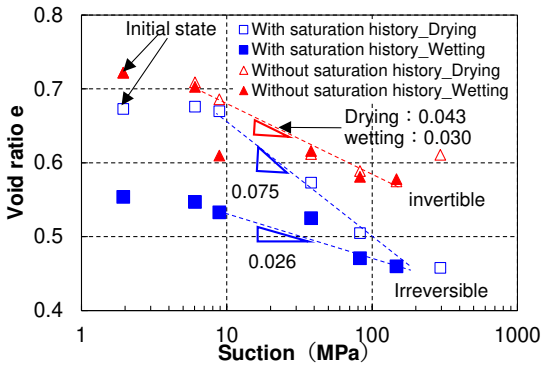

Figure 5. *Relationship of void ratio and suction*

4 NUMERICAL MODELLING OF HYDROMECHANICAL PHENOMENA IN UNSATURATED SOIL

4.1 Governing equations and water vapour diffusion in the simulations

In this study CODE_BRIGHT (Olivella et al., 1994; Olivella et al., 1996) has been used to model the hydromechanical behaviour of the clay. This code has been utilized extensively to simulate thermo-hydro-mechanical coupled problems in which expansive clays are subjected to heating and hydration, and additionally where vapour flow is relevant to water transport (Gens et al., 1998; Guimaraes et al., 2007). Only a brief description of the relevant formulation is included here. The governing equation of this code has balance equations for mass balance of solid, of water, and of air, momentum balance for the medium and internal energy balance for the medium as follows:

$$\frac{\partial}{\partial t}\left(\rho_s(1-\phi)\right) + \nabla \cdot (\boldsymbol{j_s}) = 0 \quad (1)$$

$$\frac{\partial}{\partial t}\left(\theta_l^w S_l \phi + \theta_g^w S_g \phi\right) + \nabla \cdot \left(\boldsymbol{j}_l^w + \boldsymbol{j}_g^w\right) = f^w \quad (2)$$

$$\frac{\partial}{\partial t}\left(\theta_l^a S_l \phi + \theta_g^a S_g \phi\right) + \nabla \cdot \left(\boldsymbol{j}_l^a + \boldsymbol{j}_g^a\right) = f^a \quad (3)$$

$$\nabla \cdot \boldsymbol{\sigma}_t + \boldsymbol{b} = 0 \quad (4)$$

$$\frac{\partial}{\partial t}\left(E_s\rho_s(1-\phi) + E_l\rho_l S_l \phi + E_g\rho_g S_g \phi\right) + \nabla \cdot \left(\boldsymbol{i}_c + \boldsymbol{j}_{ES} + \boldsymbol{j}_{El} + \boldsymbol{j}_{Eg}\right) = f^Q \quad (5)$$

where ρ_s, ρ_l and ρ_g are the solid, liquid and air density, respectively; ϕ is porosity, S_α is the volumetric fraction of pore volume occupied by the α-phase (liquid or gas); θ_α^β is the mass of β-species (air or water) per volume of α-phase (liquid or gas); f^w and f^a are the external mass supply of water and air, respectively, per unit volume of medium; $\boldsymbol{j}_\alpha^\beta$ is the total mass flux of β-species (air or water) in the α-phase (liquid or gas) with respect to a fixed reference system; $\boldsymbol{\sigma}_t$ is the total stress tensor; $\boldsymbol{b}$ is the vector of body forces; $\boldsymbol{i}_c$ is the conductive heat flux and $\boldsymbol{j}_{Es}$, $\boldsymbol{j}_{El}$ and $\boldsymbol{j}_{Eg}$ are the energy fluxes due to the motion of phase (in low permeability media, these fluxes may be neglected) (Gens et al., 2007).

The mass flux of water is calculated from liquid advective flux in addition to vapour advective and non-advective fluxes, resulting in:

$$\boldsymbol{J}_l^w + \boldsymbol{J}_g^w = \rho_l \boldsymbol{q}_l + \omega_g^w \rho_g \boldsymbol{q}_g - \boldsymbol{D}_g^w \Delta \omega_g^w \quad (6)$$

where ω_g^w is the mass fraction of water in the gas phase that is related to vapour density; $\boldsymbol{D}_g^w$ is the diffusion-dispersion tensor; and ω_g^w is the mass fraction of water in the gas phase that is related to vapour density:

$$\omega_g^w = \frac{\theta_g^w}{\rho_g} \quad (7)$$

the mass of water per volume of gas is calculated from equation (8) by psychrometric law and relative humidity is calculated by equation (9):

$$\theta_g^w = \left(\theta_g^w\right)_0 \cdot e^{-\frac{(P_g - P_l)\cdot M_w}{R\cdot(273.15+T)\cdot\rho_w}} \quad (8)$$

$$\mathrm{RH}(\%) = \frac{\theta_g^w}{(\theta_g^w)_0} \cdot 100 \quad (9)$$

where $\left(\theta_g^w\right)_0$ is vapour concentration in the gas phase – vapour density – at vapour saturation conditions ($P_g - P_l$=0) and depends on temperature; M_w is the molecular mass of water density; R is the gas constant; T is the absolute temperature.

Volumetric advective flux follows Darcy's law with a relative permeability dependent on degree of liquid saturation:

$$\boldsymbol{q}_\alpha = \boldsymbol{k}\frac{k_{r\alpha}}{\mu_\alpha} \cdot (\nabla P_\alpha - \rho_\alpha \boldsymbol{g}) \quad (10)$$

where $\mathbf{k}$ is the intrinsic permeability tensor; $k_{r\alpha}$ is the relative permeability of α-phase (liquid or gas); P_α is the pressure of α-phase (liquid or gas); $\mathbf{g}$ is the gravity vector.

Relative permeability of the liquid phase is defined by a power law (equation (11)) which depends on effective saturation of degree:

$$k_{rl} = (S_e)^n \ , \ S_e = \frac{S_l - S_{rl}}{S_{ls} - S_{rl}} \quad (11)$$

For relative permeability of the gas phase, the equation for the liquid phase is used:

$$k_{rg} = \left(S_g\right)^n , S_g = 1 - S_l \tag{12}$$

where S_{lr} and S_{ls} are the residual and maximum degrees of liquid saturation, respectively.
For treatment of non-advective terms (i.e., diffusive/dispersive) Fick's law has been used:

$$-\boldsymbol{D}_\alpha^\beta \nabla \omega_\alpha^\beta = -(\tau \phi \rho_\alpha S_\alpha D_\alpha^i \boldsymbol{I}) \nabla \omega_\alpha^i \tag{13}$$

where τ is the tortuosity; ρ_α is the density of α-phase (liquid or gas); S_α is the degree of saturation of α-phase (liquid or gas); D_α^i is the molecular diffusion coefficient which is a function of temperature and gas pressure and $\boldsymbol{I}$ is the identity matrix.

Variation of relative humidity by the vapour equilibrium technique in controlled-suction tests is calculated from variation of the mass fraction of water in the gas phase that is due to vapour density which is computed from psychrometric law, and the physical quantity is calculated by solving the mass flux of the liquid phase calculated from the advective term and the non-advective term, so that the mass balance of the liquid phase is satisfied.

4.2 Mechanical constitutive law

The mechanical response is described within the framework of the elastoplastic model proposed by Alonso et al. (1990). The volumetric strain is dependent on change in suction:

$$\dot{\varepsilon}_{\boldsymbol{vol}}^{\boldsymbol{e}} = \frac{\kappa(s)}{(1-e)p_{net}} \dot{\boldsymbol{p}}_{net} + \frac{\kappa_s}{(1+e)(s+p_{atm})} \dot{s} + (\alpha_0 + 2\alpha_2 \cdot \Delta T)\dot{T} \tag{14}$$

where e is the void ratio; p_{net} is the net mean stress; p_{atm} is the atmospheric pressure; s is the suction, α_0, α_2 are model parameters, where $\kappa(s)$ and κ_s are as follows:

$$\kappa(s) = \kappa_0 \left(1 + \alpha \cdot s + \alpha_l ln\left(\frac{s+0.1}{0.1}\right)\right) \tag{15}$$

$$\kappa_s = \kappa_{s0}\left(1 + \alpha_{sp}\, p_{net}/p_{ref}\right) exp(\alpha_{ss} \cdot s) \tag{16}$$

where κ_0 is the initial elastic slope for specific volume mean stress; α, α_l, κ_{s0}, α_{sp} and α_{ss} is the model parameter, and p_{ref} is the reference mean stress.

This model considers the suction axis in the yield surface of the modified Cam-Clay model (Roscoe et al., 1968):

$$F^{\boldsymbol{LC}} = J^{\boldsymbol{2}} - \frac{M^2}{3}(p_{net} + p_s)(p_0 - p_{net}) = 0 \tag{17}$$

where J is the second invariant of the deviatoric stress tensor; M is the limiting critical state line parameter; p_s and p_0 considered dependent on suction:

$$\mathrm{p}_s = p_{s0} + k \cdot s \cdot e^{-\rho_T \cdot \Delta T} \tag{18}$$

$$p_0 = p^c \cdot \left(\frac{p_0^*(T)}{p^c}\right)^{\frac{\lambda(0)-\kappa(0)}{\lambda(s)-\kappa(s)}} \tag{19}$$

where p_{s0} is the tensile strength in saturated conditions; k is the parameter that takes into account the increase of tensile strength due to suction; ρ_T is the parameter that considers decrease of tensile strength due to temperature; λ_0 is the slope of void ratio – mean stress curve at zero suction and κ_0 is the initial elastic slope for specific volume – mean stress at zero suction; p_c is the reference pressure. The temperature dependent preconsolidation stress $p_0^*(T)$ at saturation and the suction dependent compression index $\lambda(s)$ as follow:

$$p_0^*(T) = p_0^* + 2(\alpha_1 \cdot \Delta T + \alpha_3 \cdot \Delta T \cdot |\Delta T|) \tag{20}$$

$$\lambda(s) = \lambda_0\{(1-\gamma)exp(-\beta \cdot s) + \gamma\} \quad (21)$$

where p_0^* is initial preconsolidation mean stress for saturated soil; α_1, α_3, β and γ are model parameters, respectively.

Hardening law in relationship with plastic volumetric strains as follow:

$$\dot{p}_0^* = \frac{(1+e)\cdot p_0^*}{\lambda(0)-\kappa(0)} \cdot \dot{\varepsilon}_{vol}^p \quad (22)$$

The change in volume of the specimen due to the change in relative humidity can be considered by equation (16). The model parameter α_{sp} can be set to zero because the vapour equilibrium technique in controlled-suction tests is at unconstrained conditions (p_{net}/p_{ref}). If parameter α_{ss} is also zero, then only parameter κ_{s0} is required (Yamamoto et al., 2019). Therefore, using the $\kappa_{s0} = 0.043$ obtained from the vapour equilibrium technique in controlled-suction tests, the behaviour of the specimen in the target tests can be reproduced.

4.3 Numerical modelling of laboratory tests

4.3.1 Conceptual model

Target specimen for numerical modelling is a cylindrical specimen with a diameter of 60 mm and a height of 20 mm. For the numerical analysis, an axisymmetric finite element mesh with 176 nodes and 150 elements has been chosen. The unknown variables are the vertical and horizontal displacement (δ_v, δ_h), the liquid pressure(P_l). Figure 6 shows the geometry of the mesh, as well as the initial and boundary conditions. The initial conditions considered in simulation are a void ratio of 0.724, an initial saturation of 68.7% and an initial stress of 0.11MPa. The temperature was kept constant at 20 ℃. The vapour equilibrium technique in controlled-suction tests has provided the change in the relative humidity. Therefore, relative humidity is applied on the upper and side boundaries (red line in the Figure 6). The evaporation rate may be expressed with the following equation (Wilson et al., 1994).

$$j_g^w = \beta_g \left[\omega_g^w \rho_g - \left(\omega_g^w \rho_g\right)^0\right] \quad (23)$$

where $\left(\omega_g^w \rho_g\right)^0$ is the density in the environment. This equation means that the evaporation rate is proportional to the difference between vapour density in the atmosphere and vapour density on the specimen surface. The value of β_g related to the turbulence exchange function was set to 10.

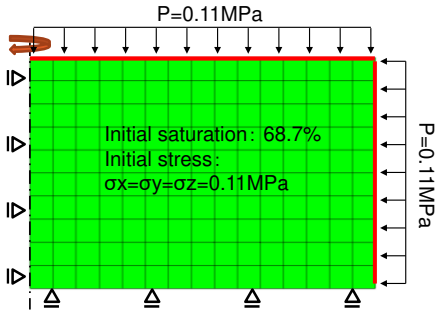

Figure 6. *Conceptual model used in the analysis of the test*

4.3.2 Model parameters

Mechanical parameters were defined based on previous research results (JNC, 1999) and are shown in Table 2. The retention curve obtained from the experiments described in section 2.2 was used. Relative permeability is calculated by equation (11), in which the value of n = 3. Figure 7 shows the retention curve and relative permeability. Note that, the analysis was performed with the air pressure held constant (P_g=0.1 MPa). The intrinsic permeability of the material was also defined on the basis of previous research results (JNC, 1999) using the effective clay density (equation (25)), sand density of particles and sand mixture rate by equation (24).

$$K = e^{-42.1+1.1447\rho_e - 2.1232{\rho_e}^2} \quad (24)$$

$$\rho_e = \frac{\rho_d(100-R_S)}{100-\rho_d\frac{R_S}{\rho_S}} \quad (25)$$

where ρ_d is the dry density of bentonite/sand mixture (ρ_d=1.6 Mg/m^3); R_s is the mixture rate of silica (R_s=30 wt%) and ρ_s is the sand density of solid particles (2.65 Mg/m^3).

In order to reproduce the behavior of the specimen during the controlled-suction tests, it is necessary to set the vapour diffusion parameters in equation (13). Therefore, diffusive parameters were defined based on previous research (Pollock, 1986). Advective and diffusive parameters are shown in Table 3.

Table 2. *Mechanical parameters*

Title	Symbol	Unit	Values
Initial dry density	ρ_d	Mg/m^3	1.60
Shear modulus	G	MPa	10.0
Swelling index	κ_0	-	0.07
Compression index	λ_0	-	0.117
Model parameter	κ_{s0}	-	0.043
Model parameter	α_{sp}	-	0.0
Critical state line parameter	M	-	0.63
Initial preconsolidation mean stress for saturated soil	p_0^*	MPa	0.90

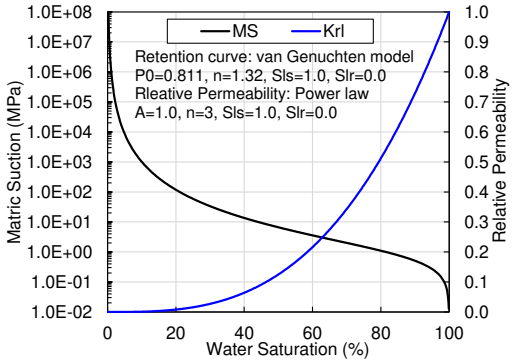

Figure 7. *Retention curve and relative permeability*

Table 3. *Advective and diffusive parameters*

Title	Symbol	Unit	Values
Intrinsic permeability	k	m^2	4.69×10^{-20}
Diffusive parameter	D	m^{2}s^{-1} K^{-n}Pa	5.6×10^{-6}
Model parameter	n	-	2.3
Coefficient of tortuosity	τ	-	1.0

4.3.3 Modelling results

CODE_BRIGHT considers coupled two-phase flow and mechanics. But in this study, gas pressure was set at P_g=0.1 MPa, and evaporation was taken into account. The relative humidity boundary conditions used in this study are shown in Figure 8. The duration of analysis steps was set to 30 days per step as in the experiment. The result of the void ratio and matric suction relationship are compared with the experiment as shown in Figure 9. The overall void ratio was calculated from the change in volume of finite element model instead of the element values. Matric suction is based on the upper and side boundary value. The void ratio - matric suction relationship show good agreement between simulation and measurement. The volume change behaviour in this study is trivially matched since it is dependent on only κ_{s0} of equation (16). However, in this analysis, relative humidity was defined as a boundary condition, and volume change behaviour related to the advection and diffusion behaviour of vapour in bentonite was solved with an unsaturated mechanical constitutive law. Volume change behaviour depends on the variation of suction as shown in equation (14), and relative humidity is also calculated

from suction as shown in equation (8) and (9). Therefore, the obtained retention curve is reasonable because the relative humidity change depends on the soil-water characteristic properties.

The evolution of relative humidity and saturation with time are shown in Figure 10. At around 10 days, the relative humidity change is observed in the figure. In the previous research, the vapour equilibrium technique in controlled-suction tests was used to obtain volume change behaviour of specimen at constant suction state (Narushima et al., 2019). According to that study, suction change reached equilibrium in 10 days to 2 weeks. Narushima et al. (2019) used crushed bentonite with dry density 1.356 Mg/m^3, while in this study compacted sodium bentonite with a 30% sand mixture and 1.6 Mg/m^3 dry density is used. The permeability behaviour of bentonite depends on the effective clay density, for that reason, the material in Narushima et al. (2019) and in this study are considered to have equivalent effective clay density. Therefore, it was assumed that the diffusivity also depends on the effective clay density, and that the target materials have the same diffusivity. Regarding the shape of the specimen, the volume, diameter and thickness are the same. From the above, the diffusion coefficient set in previous studies is assumed to be appropriate. However, in this study, for simplicity the gas pressure was fixed at P_g=0.1 MPa. In contrast, referring to the Tetens equation that defines the vapour pressure, gas pressure also changes. For example, the vapour pressure at a relative humidity of 98% is 2.283 kPa, calculated from the partial pressure of the saturated water vapour pressure. As a result, when the humidity is reduced to 11%, the vapour pressure decreases to 0.256 kPa. Therefore, in the future, it will be necessary to improve the accuracy of the analysis by considering the gas pressure.

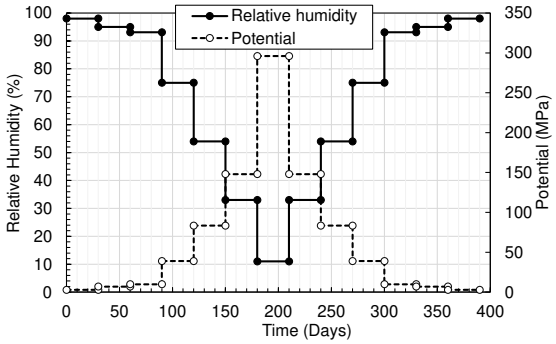

Figure 8. *Steps used in the analysis*

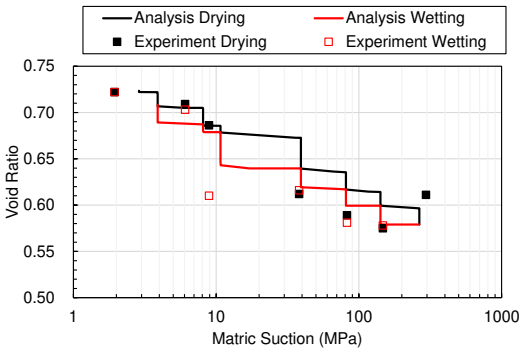

Figure 9. *Comparison of void ratio and suction from experiment and simulation*

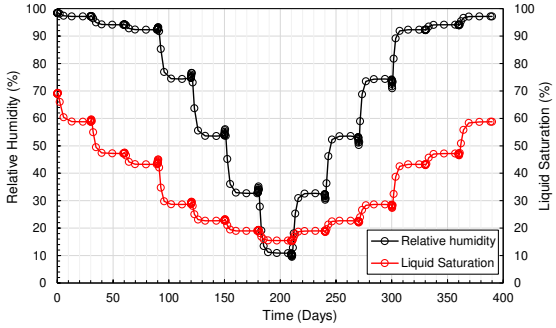

Figure 10. *Evolution of relative humidity and saturation with time in the simulation*

5 CONCLUSIONS

In this study, soil-water characteristic properties were obtained from a dew-point water potential meter and the material property variation for volume change for change in saturation were obtained from column tests for the compacted bentonite/sand mixture. Simulation of the tests was then performed using the obtained parameters, to validate the derived physical properties. The results from the study are summarized below.

In this study, a soil-water characteristic curve for compacted bentonite/sand mixture with dry density of 1.600 Mg/m^3 is determined using a van Genuchten model fitted to experimental data sets. The material properties for volume change with change in saturation for specimens with or without saturation history were obtained from column tests for the compacted bentonite/sand mixture. The specimen with

saturation history produced a large reduction in void ratio, which is significantly greater than the specimen without saturation history. Therefore, the changes in suction and void ratio during drying and wetting processes showed that bentonite without saturation history changed reversibly, and bentonite with saturation history changed irreversibly. This is thought to be due to changes in soil structure due to swelling of montmorillonite that occurred during saturation. Simulations of the experiment were in good agreement with the laboratory results, and the validity of the analysis method was confirmed. Furthermore, the validity of the model parameters for vapour diffusion was also confirmed. However, in the simulations the gas pressure was fixed at P_g=0.1 MPa for simplicity. In the future, it will be necessary to consider the change in gas pressure to improve the credibility of the analysis.

REFERENCES

Alonso, E. E., Gens, A. & Josa, A. (1990). A constitutive model for partially saturated soils. Geotechnique, 40, 405–430. 30).

Ayman A.A, Wojciech T.S. (2017). A study on how to couple thermo-hydro-mechanical behaviour of unsaturated soils: Physical equations, numerical implementation and examples, Computers and Geotechnics, Volume 92, December, 132-155

Blatz, James A., Yu-Jun Cui, and Luciano Oldecop. "Vapour equilibrium and osmotic technique for suction control." Laboratory and field testing of unsaturated soils. Springer, Dordrecht, 2008. 49-61.

Bulut R., Hineidi S.M. and Bailey B. 2002. Suction measurements—filter paper and chilled mirror psychrometer. Proceedings of the Texas Section American Society of Civil Engineers, Fall Meeting, Waco, 2–5 October.

Delage, P., M. D. Howat, and Y. J. Cui. "The relationship between suction and swelling properties in a heavily compacted unsaturated clay." Engineering geology 50.1-2 (1998): 31-48.

Qin, B., Chen, Z., Fang, Z., Sun, S., Fang, X. and Wang, J. (2010). Analysis of coupled thermo-hydro-mechanical behavior of unsaturated soils based on theory of mixtures I, Applied Mathematics and Mechanics volume 31, 1561–1576.

Collin, F., Li, X. L., Radu, P. J. and Charlier, R. (2002). Thermo-hydro-mechanical coupling in clay barriers, Engineering Geology, Volume 64, Issues 2–3, May, 179-193

Gens, A., Garcia-Molina, A., Olivella, S., Alonso, E.E., and Huertas, F. (1998). Analysis of a full scale in situ test simulating repository conditions. International Journal for Numerical and Analytical Methods in Geomechanics, 22, 515-548.

Gens, A., Garitte, B., Wileveau & Y. (2007). In situ behaviour of a stiff layered clay subject to thermal loading: observations and interpretation, Geotechnique 57, 207-228.

Guimaraes, L.D., Gens, A., and Olivella, S. (2007). Coupled thermo-hydro-mechanical and chemical analysis of expansive clay subjected to heating and hydration. Transport in Porous Media, 66, 341-372.

Japan Nuclear Cycle Development Institute (1999). Overview of safety assessment in the 2nd draft of the second progress report on research and development for the HLW disposal in Japan, JNC-TN1400-99-022, (In Japanese).

Maček, M.; Smolar, J.; Petkovšek, A. Extension of measurement range of dewpoint potentiometer and evaporation method. In: Proc. 18th International Conference on Soil Mechanics and Geotechnical Engineering. French Society for Soil Mechanics and Geotechnical Engineering (CFMS), Paris. 2013. p. 1137-1142.

Narushima, S., Arai, Y., Sakoda, Y., Nishimura, T. (2019). Understanding of swelling pressure and conductivity for an unsaturated crushed bentonite with different density, Proceedings of the 13th Japan National Symposium on Environmental Geotechnology in Sapporo, 331-334, (In Japanese).

Olivella, S., Carrera, J., Gens, A., and Alonso, E.E. (1994). Nonisothermal multiphase flow of brine and gas through saline media, Transport in Porous Media, 15, 271-293.

Olivella, S., Gens, A., Carrera, J., and Alonso, E. E. (1996). Numerical formulation for a simulator (CODE_BRIGHT) for the coupled analysis of saline media, Engineering Computations, Vol. 13, No. 7, pp.87-112.

Pintado, X., Lloret, A., and Romero, E. (2009). Assessment of the use of the vapour equilibrium technique in controlled-suction tests, Can. Geotech. J. 46, 411-423.

Pollock, D., W. (1986). Simulation of fluid flow and energy transport processes associated with high level radioactive waste disposal in unsaturated alluvium, Water Resour. Res. 22(5).

Roscoe, K. H., Burland, J. B. (1968). On the generalized stress – strain behavior of 'wet' clay, Engineering Plasticity, Cambridge University Press, 535-609.

van Genuchten and M.Th. (1980) A closed-form equation for predicting the hydraulic conductivity of unsaturated soils, Soil Sci. Soc. Am. J., 44:892-898.

Wilson, G. W., Fredlund, D. G., and Barbour, S. L. (1994) Coupled soil-atmosphere modelling for soil evaporation, Canadian Geotechnical journal, 31(2), pp.151-161.

Yamamoto, S., Sato, S., Shimura, T., Enrique, R. Nishimura, T., Oowada, H. (2019). Mechanical characteristics and water retention properties of unsaturated bentonite-based engineered barrier materials based on controlled suction tests, Journal of JSCE C (Geosphere engineering) Vol. 75, No. 3, pp257-272 (In Japanese).

Zhu, B., Ye, Z., Wang, L., Kong, D., Xu, W., Kolditz, O., Nagel, T., Chen Y. (2020). Hydro-mechanical behavior of unsaturated soil surrounding a heated pipeline considering moisture evaporation and condensation, Computers and Geotechnics, Volume 119, March.